Optimal design of temporal resolution of soft X-ray picosecond framing cameras based on micro-channel plate

Wenzheng Yang (杨文正)[1], Yonglin Bai (白永林)[1], Xiaohong Bai (白晓红)[1], Junjun Qin (秦君军)[1], Baiyu Liu (刘百玉)[2], and Bo Wang (王 博)[1]

[1]*Key Laboratory of Ultra-Fast Photoelectric Diagnostics Technology, Xi'an Institute of Optics and Precision Mechanics, Chinese Academy of Sciences, Xi'an 710119, China*

[2]*State Key Laboratory of Transient Optics and Photonics, Xi'an Institute of Optics and Precision Mechanics, Chinese Academy of Sciences, Xi'an 710119, China*

[*]*Corresponding author: ywz@opt.ac.cn*

Received December 21, 2010; accepted January 25, 2011; posted online June 27, 2011

The transit characteristics of gain electrons in the dynamic electric field in one micro-channel, the relation of the temporal resolution, and the gating electric pulse are discussed in detail. The simulation analyses provide guidance on how to select parameters of the gating electric pulse for designing the X-ray picosecond framing camera, based on micro-channel plates, especially with regard to the aspect of the temporal resolution of the camera. Certain experimental results are presented.

OCIS codes: 230.0120, 280.0280, 320.0320.
doi: 10.3788/COL201109.S10301.

The soft X-ray picoseconds framing camera (XPFC), which is based on the gated micro-channel plate (MCP), also known as MCP-XPFC, can be used as an ultrafast diagnostic tool to obtain time-resolved images with picosecond resolution in a number of applications, including the inertial confinement fusion (ICF), the laser-produced plasmas, photo-physics, photo-chemistry, and material science[1−5]. In the MCP-XPFC, when a high-voltage gating electric pulse is applied on the MCP, a curve depicting the camera gain versus the time can be obtained, and the full-width at half-maximum (FWHM) of the curve is defined as the temporal resolution of the camera. By ignoring the effects of the individual characteristic differences of MCPs, the temporal resolution and the gain of the MCP-XPFC can be found to be primarily dependent on the width and amplitude of the picosecond gating electric pulse; further, these two parameters are closely correlated with characteristics of electron transit and multiplication in the MCP[6,7].

The gain of the MCP-XPFC is proportional to the amount of gain electrons transmitting through the MCP. It is well known that both the energy and emission angle of either X-ray-induced photoelectrons or the secondary gain electrons are of certain randomness, but they also follow a probability distribution. Further, all electrons move in a dynamic electric field in the MCP. As a consequence, the amount of gain electrons transmitting through the MCP will follow a probability distribution versus transit time. Usually, the transit time for the maximum probability of the electron to transmit through the MCP is called the most probable electron transit time of MCP (simply as electron transit time $T_{\rm r}$), and the FWHM of the electron transit-time distribution curve is defined as the electron transit-time spread of the MCP (simply as electron transit-time spread TTS).

To obtain a more detailed insight and to improve operation of the MCP-XPFC, an investigation of the characteristics of the electron transit in the micro-channel of the MCP, gated by gating electric pulse of picoseconds, is absolutely necessary. The electron transit time, electron transit-time spread, and optimization analysis of temporal resolution of the MCP-XPFC with a 0.5-mm-thick MCP are discussed theoretically.

A model of the electron motion in the micro-channel of the MCP relates to two types of electrons: the X-ray-induced photoelectrons (i.e., initial electrons) and the subsequently generated secondary electrons. The probability distribution function of the emission energy ($E_{\rm k}$) of photoelectrons extracted from the gold photocathode by 0.1−10-keV X-rays is expressed by[6]

$$f(E_{\rm k}) = A\frac{E_{\rm k}}{(E_{\rm k}+3.7)^4},$$

where $E_{\rm k}$ is the maximum probability of the emission energy, and A is considered essentially as a constant to be adjusted for "best fitting".

The emission angle distribution of photoelectrons is, in general, considered to be a cosine distribution. Photoelectrons emitted from the cathode can be considered as isotropic particles and only considering trajectories of electron motion on one axial plane of micro-channel in the MCP. The probability distribution curves of both E_x and emission angle θ of initial photoelectrons were obtained by the Monte Carlo simulation. To simplify the method of calculation, only the trajectories of electron motion for the same-axis plane are considered in theoretic calculations.

For the ith random wall-to-wall transit process of the subsequent secondary electrons, we define that t_i is the moment of the ith electron bombarding the wall surface, t_{i-1} is the $(i-1)$th emission moment of secondary electrons, $\mathrm{eV}_{\mathrm{o}(i)}$ is the ith emission energy, $\mathrm{eV}_{\mathrm{r}(i)}$ is the ith radial bombarding wall energy, $\mathrm{eV}_{\mathrm{z}(i)}$ is the ith axial bombarding wall energy, $\mathrm{eV}_{(i)}$ is the ith bombarding wall energy, Z_i is the ith electron flight displacement between wall encounters, θ is the emission angle, L is the channel

thickness ($L = 0.5\times 10^{-3}$m), D is the channel diameter ($D = 12.5\times10^{-6}$ m), e is the electronic charge, and m is the electronic mass.

In general, the radial emission energy $\mathrm{eV_{or}}$ and the axial emission energy $\mathrm{eV_{oz}}$ of the electron are both considerably smaller than the axial energy gain of the electron $\mathrm{eV_z}$. The maximum probability of the emission angle is $\theta = 0°$; that is, the most number of electrons are emitted at an angle orthogonal to the channel surface. Every wall-to-wall transit in the channel for secondary electron can refer to "energy proportionality hypothesis"[7]. A similar assumed expression can be derived for the energy proportionality hypothesis as

$$\mathrm{eV_{o(}}_{i)} = \mathrm{eV_{(}}_{i-1)}/4\beta^2, \tag{1}$$

where $\beta = 2.47$ is a dimensionless proportionality constant[7].

The gating electric pulse $V_{\mathrm{m}}(t)$ is assumed to be a Gaussian electric pulse for simplicity, and is expressed by

$$V_{\mathrm{m}}(t) = V_{\mathrm{mp}} \exp[-4\ln 2(\frac{t-T_{\mathrm{n}}}{T_{\mathrm{n}}})^2], t \in [0, 2T_{\mathrm{n}}], \tag{2}$$

where V_{mp} is the amplitude of pulses and T_{n} is the FWHM of pulses.

Therefore, the t_i can be calculated by

$$t_i = t_{i-1} + D/\sqrt{(2\mathrm{eV_{or}}_{(i-1)}/m)}. \tag{3}$$

The ith bombarding wall energy $\mathrm{eV}_{(i)}$ can be obtained by

$$\mathrm{eV}_{(i)} = \mathrm{eV_{o(}}_{i)} + \frac{e^2}{2mL^2}\left[\int_{t_{i-1}}^{t_i} V_{\mathrm{m}}(t)\,\mathrm{d}t\right]^2. \tag{4}$$

For the next collision process, the emission energy $\mathrm{eV}_{\mathrm{o}(i+1)}$ can be calculated by Eq. (1). When electrons transit out of the back of the MCP, the total flight time of the electron in the channel is given by $T_{rj} = \sum_{i=1}^{n} t_i - t_0$, where n is the collision number and j is the sample number of the electron.

By using a statistical histogram to analyze all T_{rj}, the maximum probability of T_{rj} distribution is defined as the most probable electron transit time T_r of the MCP and the FWHM value of the statistical distribution is defined as the TTS of the MCP.

In the experiment, a set of electrical pulses with duration ranging from 170 to 250 ps and amplitude between 2 and 3 kV are applied on the MCP-XPFC. The characteristic impedance of micro-strips on the MCP is approximately 13−16 Ω. Therefore, amplitudes of the electric pulse need to be in the range of 800–1200 V to drive the micro-strip lines of the MCP-XPFC. In this letter, a pulse width of 170−260 ps and pulse amplitude of 800–1500 V are taken into account in calculations.

Certain conclusions with regard to the electron transit-time characteristics can be obtained from Fig. (1):

1) A narrow pulse width and large pulse amplitude can decrease the electron transit time.

2) The pulse amplitude has a sharper influence on the electron transit time than on the pulse width.

3) With increase in the pulse width, a tendency to be close to the linear change is observed when plotting the electron transit time against the pulse amplitude.

4) The pulse width has an inconspicuous influence on the electron transit time at high-voltage segments of the curves. From Fig. 1, values of the electron transit time are approximately equal with a pulse width of 210−260 ps at 1 500 V.

Conclusions obtained from Fig. (2) with regard to the electron transit-time spread characteristics include:

1) A large pulse amplitude can decrease the electron transit-time spread.

2) The pulse amplitude has a sharper influence on the electron transit-time spread than on the pulse width.

3) With the increase in the pulse amplitude, the electron transit-time spread of the narrower pulse decreases more conspicuously than the wider pulse.

4) The electron transit-time spread curves intersect at approximately 62 ps at a voltage of 1 000 V.

Based on the conclusions obtained from Figs. 1 and 2, gating pulses with characteristics such as amplitude higher than 900 V and across a 200- to 250-ps pulse envelope develop the ability to be applied to the MCP when used in the framing camera in engineering applications. Further, the resolution of the MCP-XPFC is within the range of 60−80 ps in theory.

The simulation results of the influence of the gating pulse's width and amplitude to the temporal resolution of the XFC are presented in Fig. 3.

A narrow pulse width and larger pulse amplitude can improve the temporal resolution because of the resultant decrease in the electron transit-time spread. The minimum temporal resolution of the camera is determined primarily by the electron transit-time spread; further, the larger pulse amplitude can decrease the electron transit-time spread. Therefore, the temporal resolution of a camera can be improved by increasing the gating voltage, and by other such methods. However, larger pulse amplitudes, such as 1 300–1 500 kV required to drive the micro-strip lines of the MCP-XPFC, cannot improve the temporal resolution for gain saturation absorption of the MCP, as shown in Fig. 3.

In the application of the abovementioned conclusions to select parameters of the gating electric pulse, attention to the interaction of the pulse width and the pulse amplitude on the temporal resolution is warranted, and

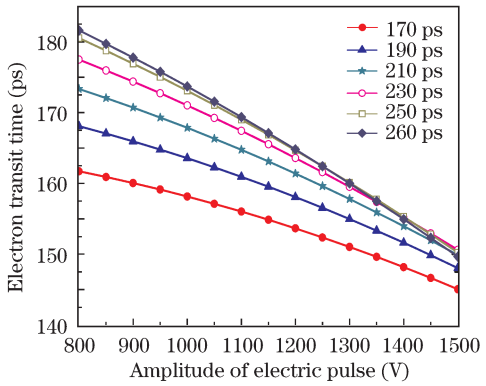

Fig. 1. Change curves of electron transit time versus pulse amplitudes with different pulse widths.

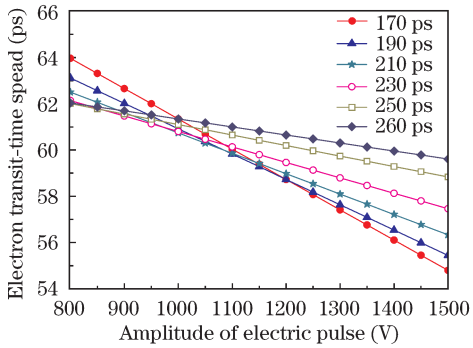

Fig. 2. Change curves of electron transit-time spread versus pulse amplitudes with different pulse widths.

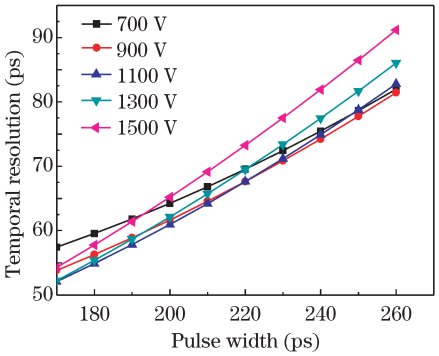

Fig. 3. Change curves of temporal resolution versus pulse widths with different pulse amplitudes.

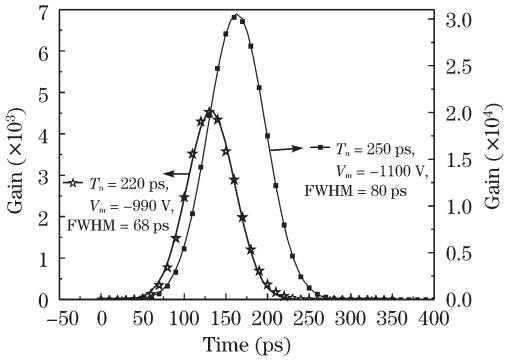

Fig. 4. Simulation gain curves of MCP-XPFC with two gating pulses.

it is very important to optimize the MCP-XPFC.

In the present experiment, as the temporal resolution of the MCP-XPFC can be improved by decreasing the width pulse of the gating pulse by applying a bias voltage, we get

$$V_{\mathrm{B}}(t) = V_{\mathrm{m}}(t) + V_{\mathrm{bias}}$$

$$= -V_{\mathrm{m}} \exp\left[-4\ln 2(\frac{t-T_{\mathrm{n}}}{T_{\mathrm{n}}})^2\right] + V_{\mathrm{bias}}, \quad (5)$$

where $V_{\mathrm{m}}(t)$ is initial gating pulse and V_{bias} is the bias voltage. Electric pulses of 250 ps at a voltage of −2 500 kV are usually applied on the MCP-XPFC. Theoretically, amplitudes of the electric pulse need to be approximately −1 100 V to drive the micro-strip lines and the temporal

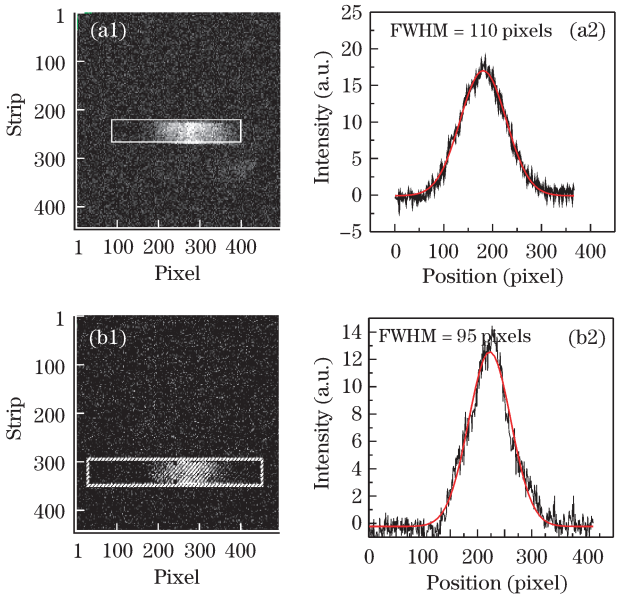

Fig. 5. Experimental images and intensity curves of camera with two gating pulses. (a): T_{n} = 250 PS, V_{m} = −1100 V; (b): T_{n} = 220 ps, V_{m} = −900 V.

resolution needs to be approximately 78.8 ps. If the 200-V bias voltage is applied to the MCP, the gating pulse required to drive the micro-strip lines is 220 ps with a voltage of −900 V and the theory temporal resolution needed is approximately 68 ps. Two gating pulses, of 250 and 220 ps with a voltage of −1100 and −900 V, respectively, are selected for calculations, and the results are shown in Fig. 4.

A 248.5-nm krypton fluoride (KrF) laser was used as the light source for the camera photocathode. The laser produced 500-fs pulses emitting 5-mJ/pulse energy at a repetition rate of 1 Hz. The average energy per pulse impinging on the MCP in each beam was approximately 3 mJ. The output image of the camera was captured by using a charge-coupled device (CCD) camera, which was used to view the fiber-optic faceplate of the phosphor screen. The integrated intensity versus the CCD image pixel number illustrates the variation in gain, and its FWHM indicates the temporal resolution T_e of the MCP-XPFC, which is calculated by[6]

$$T_e = \mathrm{FWHM}_{\mathrm{GG}}/(v \times P_x), \quad (6)$$

where $\mathrm{FWHM}_{\mathrm{GG}}$ is the FWHM of the integrated intensity curve, v is the propagation speed of the gating pulses, and P_x is the number of pixels per millimeter. The values of v and P_x are measured as v = 0.18 mm/ps and P_x = 33.3 pixels/mm, and T_{e} is calculated by using Eq. (6)[8]. The experimental results are shown in Fig. 5 and they are in accord with the simulation results shown in Fig. 4.

In conclusion, the discussion of transit time and time-spread characteristics of the gain electrons in the dynamic electric field of a micro-channel are discussed on the basis of certain assumptions and parameters. The conclusion obtained from analyses of simulation results guide the selection of parameters of the gating pulse for designing the MCP-XPFC, especially with regard to the temporal resolution of the camera. However, it is

necessary that the actual conditions for optimizing the design of the MCP-XPFC, such as the parameters of the MCP (thickness, L/D ratio, the percentage of pore area, material characteristics of MCP, etc.), the structure of the framing tube (proximity distance, property of photocathode, the number of MCP, etc), the characteristic requirements of the MCP-XPFC (temporal resolution, spatial resolution, electronic gain, etc.), the design and making of the electrical pulse production and other similar factors be taken into account.

References

1. D. K. Bradley, P. M. Bell, J. D. Kilkenny, R. Hanks, O. Landen, P. A. Jaanimagi, P. W. McKenty, and C. P. Verdon, Rev. Sci. Instrum. **63,** 4813 (1992).
2. F. Ze, R. L. Kauffman, J. D. Kilkenny, J. Wielwald, P. M. Bell, R. Hanks, J. Stewart, D. Dean, J. Bower, and R. Wallace, Rev. Sci. Instrum. **63,** 5124 (1992).
3. Z. Chang, B. Shan, X. Q. Liu, and B. Shan, Acta Photon. Sin. (in Chinese) **24,** 501 (1995).
4. M. Koga, T. Fujiwara, T. Sakaiya, M. Lee, K. Shigemori, H. Shiraga, and H. Azechi, Rev. Sci. Instrum. **79,** 10E909 (2009).
5. M. Katayama, M. Nakai, T. Yamanaka, Y. Izawa, and S. Nakai, Rev. Sci. Instrum. **62,** 124 (1991).
6. L. H. Burton and A. S. Jerel, J. Appl. Phys. **48,** 1852 (1977).
7. E. H. Eberhardt, Appl. Opt. **18,** 1418 (1979).
8. W. Yang, Y. Bai, B. Liu, J. Zhao, and X. Bai, Acta Electron. Sin. (in Chinese) **37,** 603 (2009).